PHILIPPINE ENGINEERING JOURNAL
PEJ 2022; Vol. 43, No. 1: 23-46

Received: 19 October 2021
Accepted: 6 February 2022

Assessing the Effects of Different Typhoon Tracks on Storm Surge Generation in Manila Bay using ADCIRC

Imee Bren O. Villalba, Eric C. Cruz and Andrei Armani A. Adame
Institute of Civil Engineering, College of Engineering,
University of the Philippines, Diliman, Quezon City, Philippines

Abstract — *Manila Bay is an important semi-enclosed bay in the Philippines that is considered vulnerable to storm surges due to its shallow bathymetry and exposure to typhoons. To help in coastal disaster assessment, this paper investigates the effects of different typhoon tracks on storm surge generation in Manila Bay. A storm surge model was developed for Manila Bay using the Advanced Circulation (ADCIRC) model. The model was validated using the observed data during Typhoon Rammasun (Glenda) 2014. From analysis of historical typhoon tracks, three (3) major group of typhoon track directions were considered in this study – namely, due Northwest (NW), due West (W), and due Southwest (SW). The synthetic tracks per direction group were created from historical tracks and shifting the tracks vertically, creating a total of 5 tracks per direction. The tracks were then simulated using the intensity of the calibrated Typhoon Rammasun 2014. It is found that NW tracks produced higher peak surges compared to W and SW tracks, and the due Northwest track traversing near the center of the bay (NW3 track) produced the highest peak storm surges. Also, shifting the tracks along the latitude affected the magnitude and duration of storm surges along the coast. Highest peak storm surges for all the tracks were located at the northern portion of the bay along the coasts of Pampanga and Northern Bataan. In Bacoor Bay, peak surges occurred first than peak surges in other coastlines. Different windspeeds of 80, 100, and 120 knots were also simulated using NW3 track resulting to corresponding highest water levels of 4.5 m, 5.0 m, and 6.7 m, respectively. The results of the study highlight that the characteristics of peak storm surge variation along the coasts of Manila Bay are influenced by the bathymetry, coastline orientation, and shape of the bay.*

Keywords — ADCIRC, Manila Bay, storm surge, Typhoon Rammasun, typhoon tracks

I. INTRODUCTION

In the Philippines, storm surge is one of the major causes of coastal disasters. Located in the very active Western North Pacific typhoon basin, the country receives an average of 19.4 tropical cyclones (TCs) entering the Philippine Area of Responsibility and nine (9) landfalling TCs every year [1]. In 2013, Typhoon Haiyan (Yolanda) generated a storm surge of 5-7 m in San Pedro Bay which caused loss of 6,300 lives, most of which were due to drowning and trauma [2]. While there were already efforts from the government to increase its preparedness and awareness against natural disasters during that time, one of the key problems identified was that people were not able to clearly understand the phenomenon of a storm surge [3].

Manila Bay is one of the most important bodies of water in the Philippines. It is a semi-enclosed bay in the western part of Luzon facing the West Philippine Sea. It is bounded by the provinces of Bataan, Pampanga, Bulacan and Cavite and Metro Manila (Figure 1). It is also home to the biggest port in the country. The coastal areas around Manila Bay can be regarded as susceptible to storm surges as the bay is located along the track of major storms and has a

shallow depth with an average of 20 m over a surface area of around 1,800 sq. km. In addition, a vulnerability analysis presented by Perez et al. (1999) explained that densely populated areas of Malabon and Navotas in Metro Manila, as well as the areas of Limay and Orani, Bataan are vulnerable to intense storm surges [4].

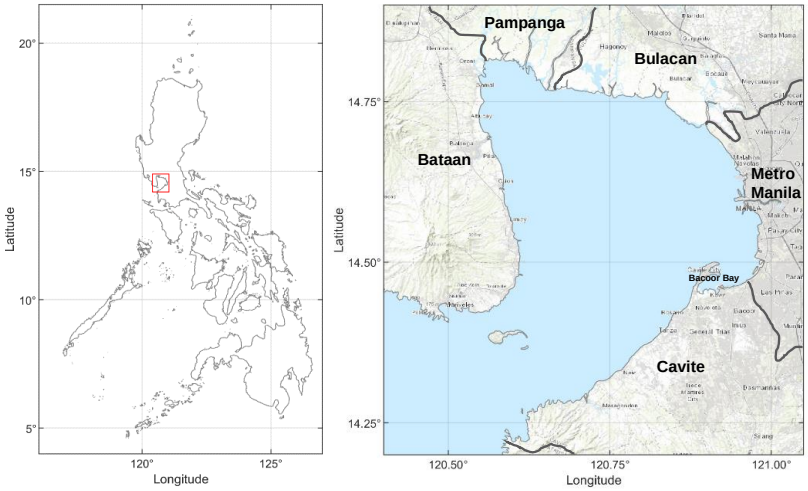

Figure 1. Study Area

Storm surge is the abnormal rise of water during the passage of a storm, over and above the predicted astronomical tides [5]. The factors that influence the maximum potential storm surge in a coastal area include the storm intensity, forward speed, angle of approach to the coast, central pressure, shape and characteristics of coastal features, and width and slope of the continental shelf [5]. Increasing storm intensity and size result in greater surge volumes [6]. The near coast storm surge characteristics depend on the size and bathymetry of the bay [7] and the storm surge height is amplified with shallow coastal bathymetry and coastal complexity [7][8][9]. A longer fetch will produce higher storm surge, but the effects to storm surge is complex and dependent on the local geography [8]. Several studies showed that typhoon tracks affect the storm surge distribution along the coastline [10][11][12]. A study by Tajima et. al (2016) observed that shifting the track of Typhoon Haiyan northward and southward affects the asymmetric distributions and timing of storm surge heights along the east and west coast of San Pedro Bay [13]. Islam and Takagi (2020) performed analysis on the sensitivity of storm surges to typhoon tracks in Tokyo Bay and found that typhoons parallel to the axis of the bay produce higher water levels in the upper bay area but the coasts adjacent to the mouth are more vulnerable to westerly tracks [14].

Several researchers have performed numerical modelling of storm surges in Manila Bay. The studies of Morin et. al (2016) and Camelo et. al (2017) focused on storm surges along Metro Manila [15][16]. A study by Lapidez et al. (2015) simulated peak storm surges reaching 4 m and above in Manila Bay by simulating the historical tracks from 1948-2013 using the strength of Typhoon Haiyan 2013 and implementing the JMA storm surge model [17]. The impact of changing typhoon tracks to storm surges in Manila Bay has not been studied. Several previous studies suggest that different typhoon tracks affect the storm surge distribution along

the coast. Having a high frequency of exposure to typhoons [1], this study postulates critical effects of different typhoon tracks on storm surges along Manila Bay.

In this study, a storm surge model was developed for Manila Bay using the Advanced Circulation (ADCIRC) Model. The ADCIRC model is an open-source program that is widely used in storm surge and coastal inundation studies [18][19][20][21]. It uses an unstructured flexible mesh that can model complex coastlines. The ADCIRC model was validated using the observed data of Typhoon Rammasun (local name Glenda) 2014. From the analysis of historical typhoon tracks, three directions of typhoon paths crossing the Manila Bay area were considered, namely due Northwest (NW), due West (W), and due Southwest (SW). We patterned the representative tracks per direction using historical typhoon tracks and developed synthetic typhoon tracks by shifting the tracks vertically, creating a total of 5 tracks per direction. Then, the tracks were simulated using the intensity of the calibrated Typhoon Rammasun 2014. The results of this study will be helpful in improving the understanding of storm surge generation in Manila Bay and may serve as a reference for coastal disaster assessment and in the planning of mitigation strategies along the coasts of the bay.

II. METHODS AND DATA

2.1 Model Description

2.1.1 Advanced Circulation (ADCIRC)

The Advanced Circulation (ADCIRC) model, developed by Leuttich and Westerink, was used to model the tides and storm surges in Manila Bay [22]. The ADCIRC-2DDI (two-dimensional depth-integrated) model, which is a continuous-Galerkin, finite element model based on the depth-integrated equations of mass and momentum equations [23], was implemented in this study. The governing equations in spherical coordinates are as follows:

$$\frac{\partial \zeta}{\partial t} + \frac{1}{R\cos\varphi}\left[\frac{\partial UH}{\partial \lambda} + \frac{\partial (VH\cos\varphi)}{\partial \varphi}\right] = 0, \tag{1}$$

$$\frac{\partial U}{\partial t} + \frac{1}{R\cos\varphi} U\frac{\partial U}{\partial \lambda} + \frac{1}{R} V\frac{\partial U}{\partial \varphi} - \left[\frac{\tan\varphi}{R} U + f\right] V = -\frac{1}{R\cos(\varphi)}\frac{\partial}{\partial \lambda}\left[\frac{p_s}{\rho_0} + g(\zeta - \alpha\eta)\right] + \frac{\nu_T}{H}\frac{\partial}{\partial \lambda}\left[\frac{\partial (UH)}{\partial \lambda} + \frac{\partial (VH)}{\partial \varphi}\right] + \frac{\tau_{s\lambda}}{\rho_0 H} - \frac{C_f\left(U^2+V^2\right)^{\frac{1}{2}}}{H} U, \tag{2}$$

$$\frac{\partial V}{\partial t} + \frac{1}{R\cos\varphi} U\frac{\partial V}{\partial \lambda} + \frac{1}{R} V\frac{\partial V}{\partial \varphi} - \left[\frac{\tan\varphi}{R} U + f\right] U = -\frac{1}{R}\frac{\partial}{\partial \varphi}\left[\frac{p_s}{\rho_0} + g(\zeta - \alpha\eta)\right] + \frac{\nu_T}{H}\frac{\partial}{\partial \varphi}\left[\frac{\partial (VH)}{\partial \lambda} + \frac{\partial (VH)}{\partial \varphi}\right] + \frac{\tau_{s\varphi}}{\rho_0 H} - \frac{C_f\left(U^2+V^2\right)^{\frac{1}{2}}}{H} V, \tag{3}$$

where t is time; λ and φ are longitude and latitude, respectively; ζ is the free surface elevation relative to the geoid; U and V are depth-integrated horizontal and vertical components of

velocity; H is the total water depth, $H = \zeta + h$, where h is the bathymetric depth relative to the geoid; f is the Coriolis parameter, $f = 2\Omega sin\varphi$, where Ω is the angular speed of the Earth; p_s is the atmospheric pressure at free surface; α is the effective Earth elasticity factor; ρ_o is the reference density of water; g is the acceleration due to gravity; respectively; η is the Newtonian equilibrium tide potential; R is the mean radius of the Earth; $\tau_{s\lambda}$ and $\tau_{s\varphi}$ are longitudinal and latitudinal components of free surface shear stress; C_f is the bottom friction coefficient; and ν_T is the depth-averaged horizontal eddy viscosity. To compute the wind stress from the wind velocity, the Garatt's formula is used [24].

2.1.2 Holland 1980 Typhoon Model

The rise of the water level during the passage of a typhoon is attributed to the surface wind stress and pressure gradient. As such, it is important in storm surge modeling to generate the wind field and pressure field of a typhoon. For limited typhoon information, an analytical/parametric model can be used to derive the pressure and wind distribution. In this study, the Holland 1980 typhoon model was used [25]. The Holland 1980 model for pressure distribution (Eq. 4) and wind distribution (Eq. 5) are described as follows:

$$p(r) = p_c + (p_n - p_c)e^{-\left(\frac{A}{r^B}\right)}, \tag{4}$$

$$V(r) = \left[\left(\frac{R_{mw}}{r}\right)^B e^{1-\left(\frac{R_{mw}}{r}\right)^B} V_{mw}^2 + \left(\frac{r^2 f^2}{4}\right)\right]^{0.5} - \frac{rf}{2}, \tag{5}$$

where r is the distance from the center of the typhoon; V is the gradient wind at radius r; p is the pressure at radius r; p_c is the central pressure; p_n is the ambient pressure; R_{mw} is the radius of maximum wind speed; V_{mw} is the maximum wind speed; f is the Coriolis parameter; and A and B are scaling parameters, given by:

$$A = R_{mw}^B, \tag{6}$$

$$B = \rho e \frac{V_{mw}^2}{P_n - P_c}, 1 < B < 2.5, \tag{7}$$

here ρ is the density of air. The parameter B defines the shape of the profile and A determines its location relative to the origin. Realistic range of parameter B are taken to be between 1 and 2.5 (Eq. 7). Increasing B makes the pressure profile to concentrate the drop near the R_{mw}, which leads to stronger winds near the R_{mw} and weaker winds at larger radii [25].

The Holland 1980 model is widely used and is capable of satisfactorily producing wind results given accurate tropical cyclone parameters [26]. Also, this model is an analytical/parametric model that is best to calculate wind fields in the inner part of the typhoon and less accurate in the outer part of the typhoon [27]. This model is applicable for this research since the selected typhoon tracks traversed the study area where the typhoon inner wind fields directly influence the storm surge generation in the bay. While the Holland 1980 model is

simple and generates wind field from a few typhoon parameters, it has limitations because it is an axisymmetric model and an actual typhoon is rarely axisymmetric [28][29].

2.2 Model Development and Parameters

To create the computational domain of the ADCIRC model for Manila Bay, the coastline data and bathymetric data are needed. The coastline of the model was generated by digitizing the coast using the Google Earth Pro [30]. The bathymetric data of Manila Bay was derived from the bathymetric data of the National Mapping and Resource Information Authority (NAMRIA) surveyed from 2016-2018. This surveyed data has a resolution of around 90-200 m and is available for the bay area up to the mouth of the bay only (Figure 2). The bathymetric data from the mouth of the bay to the specified open ocean boundary of the model domain was obtained from the General Bathymetric Chart of the Oceans (GEBCO) which has a resolution of 15 s or approximately 500 m [31].

Figure 2 shows the generated bathymetry in the model domain from 0-100 m below mean sea level and the coastline features of the bay. The shape of Manila Bay is narrow at the entrance and becomes wider at the inner bay. The entrance of the bay is oriented towards the southwest. The coastline of the bay can be described into three parts – (1) Bataan coastline (2) Pampanga-Bulacan-Metro Manila coastline which is facing the mouth of the bay and is perpendicular to the principal axis of the bay, and (3) Cavite coastline. The bathymetry of Manila Bay is relatively shallow with an average depth of 20 m. The maximum depth can be found at the entrance of the bay near Corregidor Island, and it becomes shallower at the inner bay. The general coastal slope along Bataan and Cavite coastlines can be described as steep near the entrance and becomes mild towards the inner bay. Meanwhile, the coastal slope along Pampanga-Bulacan-Metro Manila is mild and is along the principal axis. The shallowest part of the bay can be found in the northern portion of the bay (Pampanga and Northern Bataan coasts) where the coastline has a funneling shape. A special coastal feature inside Manila Bay is the Bacoor Bay which has an entrance oriented towards the northeast.

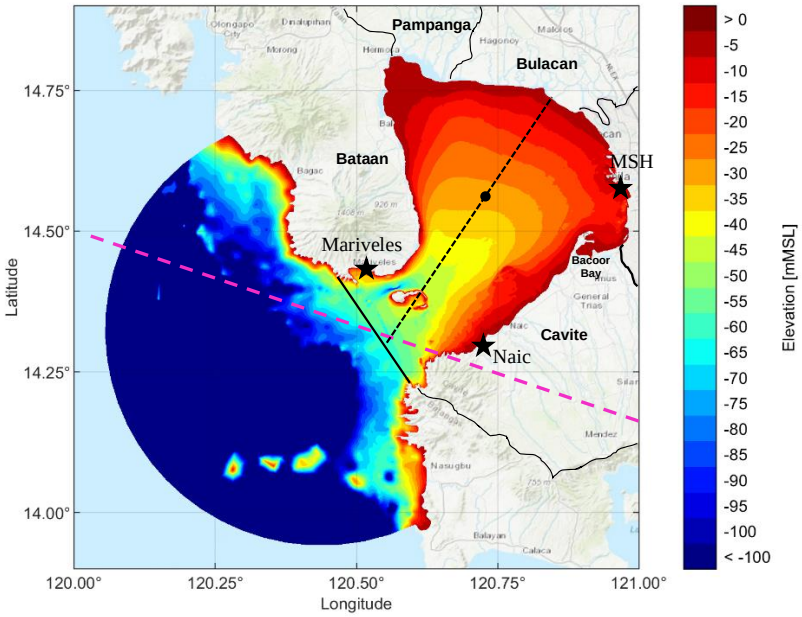

Figure 2. Map showing the bathymetry of Manila Bay, the locations of DOST-ASTI stations at Naic, Cavite and Mariveles, Bataan, the NAMRIA tide station at Manila South Harbor (MSH) and the track of Typhoon Rammasun (Glenda) 2014 (pink dashed line). Black solid line is the limit of the surveyed bathymetry of Manila Bay from NAMRIA. Black dashed line is the approximated principal axis of the bay and black dot is the approximated geometric center of the bay.

The model domain is an unstructured triangular mesh that was created using the paving technique. The computational domain covers the Manila Bay and part of the West Philippine Sea, extending from 13.94° - 14.81° latitude and 120.05° - 120.98° longitude. It has a resolution of 90 – 100 m at the coastline to 4.5 km at the open ocean boundary. The mesh has a total of 107,809 nodes and 212,081 unstructured triangular elements. Figure 3 shows the extent of the domain and the boundaries of the computational grid.

In this study, the recently released ADCIRC version 55.00 model was implemented [21]. In the ADCIRC-2DDI, the finite amplitude, advective and time derivative terms were activated. The lateral viscosity was set at 2.0 m^2/s. The Generalized Wave-Continuity Equation (GWCE) weighting factor (tau0) was specified at -1.0, in which the factor is spatially varying but constant in time. The wave equation time weighting factors were set to 0.350, 0.300, and 0.350. For the bottom friction computation, the hybrid nonlinear bottom friction law was used. The Manning's bottom roughness coefficient was set to 0.02 [32]. In the simulation of storm surge, the model time step for ADCIRC was one second and the ramping time was set to one day. The recoding time step for both astronomical tides and storm tides was 15 minutes. Then, the specified typhoon tracks were simulated during the time of Typhoon Rammasun from July 14-19, 2014.

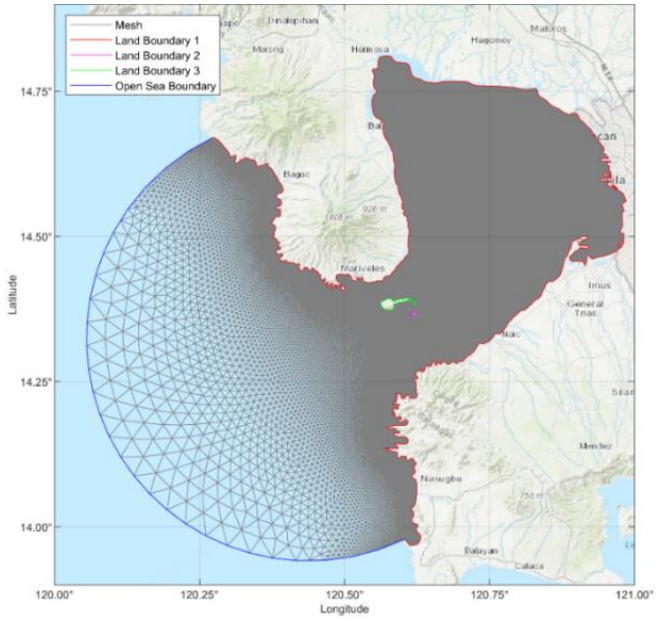

Figure 3. The ADCIRC model domain of Manila Bay with unstructured triangular mesh used in this study.

2.3 Model Validation

2.3.1 Validation of Tides

To calculate the simulated storm surge, the simulated astronomical tide is subtracted from the simulated water level (storm tide). Thus, it is important that the astronomical tide is modeled accurately. In the evaluation of the performance of the model in simulating the tide, the simulated tide was compared with the observed water level at the Manila South Harbor (MSH) station (Figure 2) of the National Mapping and Resource Information Authority (NAMRIA) [33]. To simulate the tide, tidal constituents were defined at the open ocean boundary of the ADCIRC model domain. The open ocean boundary forcing was specified with 8 main astronomical constituents K_1, K_2, M_2, N_2, O_1, P_1, Q_1, and S_2 [34] obtained from the global barotropic tide model TPXO8 developed by the Oregon State University [35]. The tide was simulated for the non-storm days [33] on April 1-30, 2019. Figure 4 shows the simulated astronomic tide generated by ADCIRC and the observed water level at the NAMRIA Manila South Harbor (MSH) station. The figure clearly shows that the model can simulate the tide levels and phase at the MSH station. The computed root-mean-squared error (RMSE) is 0.05 m, and the correlation is 0.98 which shows a good agreement with the observed tides [35].

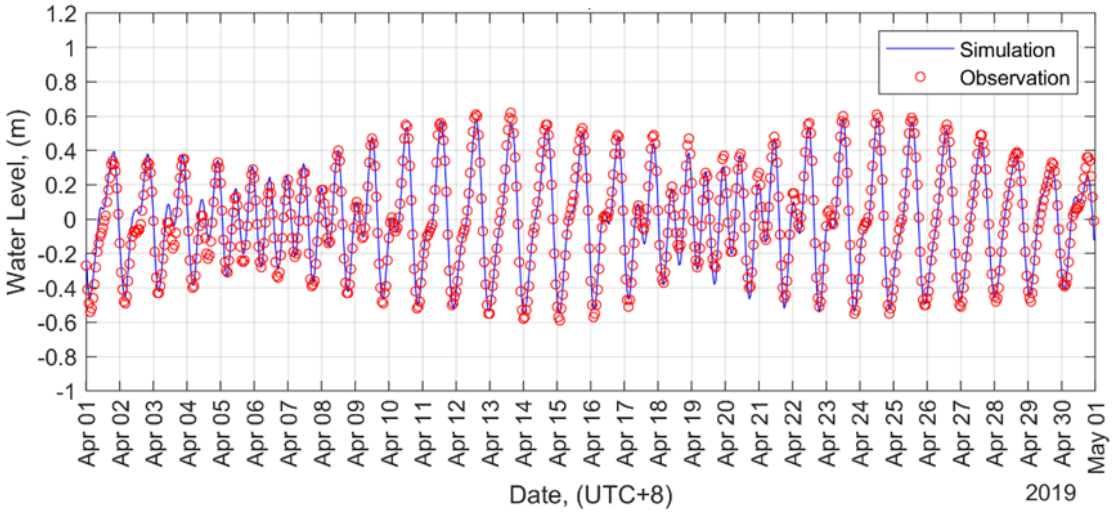

Figure 4. Comparison of the simulated tide (solid line) and observed water level (circle) at the NAMRIA Station, Manila South Harbor on April 1-30, 2019.

2.3.2 Validation of Pressure and Wind Field

A study by Camelo et al. (2017) presented the analysis of critical historical typhoons within a 150 km search radius centered in Roxas Boulevard along Manila Bay [16]. They found that Typhoon Rammasun 2014 (local name Glenda) yielded the highest storm tide and second highest storm surge, next to Typhoon Xangxane 2008. Typhoon Rammasun entered the Philippine Area of Responsibility (PAR) in the afternoon of July 13, 2014 and exited the PAR on July 17, 2014. It crossed the Bicol Region, Southern Tagalog Provinces, and Bataan. While inside the PAR, it has attained 150 kph maximum sustained windspeed [36]. It traversed the mouth of Manila Bay on July 16, 2014 towards the northwest direction (Figure 2). For this study, Typhoon Rammasun 2014 was selected to be the reference typhoon for the typhoon intensity because (1) it was considered one of the critical historical typhoons that crossed Manila Bay and (2) observed wind and pressure data were available for the calibration of the typhoon wind and pressure field. The calibrated parameters of Typhoon Rammasun 2014 were used as the typhoon intensity in the simulation of the different typhoon tracks and the corresponding storm surges in Manila Bay.

2.3.2.1 Wind model input data

The pressure and wind field of Typhoon Rammasun 2014 was generated using the Holland 1980 model and the typhoon parameters that were used in the simulation were based on the Joint Typhoon Warning Center (JTWC) best track data [37]. The JTWC best track data format can be used in the meteorological forcing file of ADCIRC (fort.22) for the symmetric vortex model (NWS=8) option. The data includes the typhoon central pressure, 1-min sustained maximum windspeed at 10-m, and the radius of maximum windspeed at 6-hour intervals. The JTWC typhoon intensities are mainly estimated based on the Dvorak model which is considered to be less accurate than in-situ measurements [38]. In addition, the 6-hourly typhoon positions of the data are only reported up to 0.1 degree of latitude and longitude.

2.3.2.1 Observed wind and pressure data

The observed wind and pressure data were obtained from the automatic weather stations (AWS) of the Department of Science and Technology – Advanced Science and Technology Institute (DOST-ASTI) [39]. The wind and pressure data of DOST-ASTI for Typhoon Rammasun 2016 were only available at stations located in Naic, Cavite (14°18'59.4" N, 120°44'43.19" E) and Mariveles, Bataan (14°26'8.1" N, 120°29'57" E). These stations are located along the coast near the mouth of Manila Bay, as shown in Figure 2. The DOST-ASTI data contains atmospheric pressure and 10-minute sustained windspeed at 2-m above the ground recorded at 15-minute intervals [40]. The observed wind data were then converted to the 10-m elevation using the power-law equation [41]. Observed minimum pressure and maximum 10-minute sustained windspeed at 10-m elevation at Naic, Cavite station during the passage of Typhoon Rammasun 2014 were 983.2 hPa and 24.8 m/s (89 kph), respectively. While in Mariveles, Bataan station, the observed minimum pressure and maximum 10-min sustained windspeed reached 984.0 hPa and 23.5 m/s (85 kph).

2.3.2.1 Calibration of the typhoon wind field and pressure field

Initially, the wind field and pressure field of Typhoon Rammasun 2014 were simulated using the typhoon parameters from the JTWC best track data. The track of Typhoon Rammasun when it traversed Manila Bay was very close to the stations in Naic, Cavite and Mariveles, Bataan (Figure 2). Thus, it was expected that observed pressures in these stations closely represent the central pressure of the typhoon. However, it is clearly shown in Figure 5a and 5c that the observed pressure deficits were lower than the simulated pressure deficits in both Naic and Mariveles stations. Using the default JTWC best track data overestimated the pressure drop and windspeeds as compared to the observed values at Naic, Cavite and Mariveles, Bataan stations (Figure 5) and there is a need to calibrate the typhoon parameters to closely match the observed values. Therefore, the typhoon input parameters were iteratively modified within a reasonable range from the original reported value until a close match was obtained between the modelled and measured data [42]. In this study, several simulation trials were done by modifying the typhoon central pressure, maximum windspeed and radius of maximum windspeed in the JTWC best track data until the simulated pressure and wind, especially the maximum windspeed, were reasonably close to the observed values.

Table 1 shows the default and modified typhoon parameters of the JTWC best track data. In the table, P_n -P_c (ΔP) is the pressure deficit, V_{mw} is the 1-minute maximum sustained windspeed and R_{mw} is the radius of maximum wind for the typhoon positions that directly affect the pressure and windspeed in Manila Bay. The modified windspeeds indicate that Typhoon Rammasun 2014 transitioned from Typhoon category (73-137 knots) to Severe Tropical Storm (55-72 knots) as characterized under the Philippine Atmospheric Geophysical and Astronomical Services Administration (PAGASA) typhoon classification when it traversed the Manila Bay area [43].

Table 1. Typhoon parameters of the default and modified JTWC best track data

	Default JTWC best track data			Modified JTWC best track data		
Date and Time (UTC+8)	P_n-P_c (ΔP) (hPa)	V_{mw} (knots)	R_{mw} (nm)	P_n-P_c (ΔP) (hPa)	V_{mw} (knots)	R_{mw} (nm)
7/15/2014 20:00	76	115	15	53	92	15
7/16/2014 4:00	69	105	12	48	75	20
7/16/2014 12:00	57	90	20	33	66	20
7/16/2014 20:00	50	80	20	33	66	20
7/17/2014 4:00	50	80	20	33	66	20

Time series comparisons of simulated and observed pressure deficit and windspeed at Naic, Cavite station and Mariveles, Bataan station are shown in Figure 5b and 5d, respectively. Surface pressures were analyzed as pressure deficits [44]. The generated pressure deficits using the modified JTWC best track agreed well with the shape of the observed values in both Naic, Cavite (Figure 5a) and Mariveles, Bataan (Figure 5c) stations. With regards to the windspeed, the simulated windspeed using the modified JTWC best track overestimated the observed windspeed in Naic, Cavite especially when the typhoon moved away from the station (Figure 5b). Nevertheless, the modified JTWC track was able to get the shape of the observed values at the Mariveles, Bataan Station (Figure 5d). The calculated root-mean-squared error (RMSE) for the observed pressure deficits and simulated values using the modified JTWC track at Naic Cavite and Mariveles, Bataan stations for the time period July 15, 12 AM to July 18, 12 AM were 3.46 hPa and 3.44 hPa, respectively. In addition, the RMSE for the observed windspeed and simulated values using the modified JTWC best track at Naic, Cavite and Mariveles, Bataan stations were 5.1 mps and 4.8 mps, correspondingly. The simulated peak wind speeds were overestimated by 7% and 13% at Naic, Cavite and Mariveles, Bataan, respectively. The discrepancies in the comparison of modeled and observed wind speeds may be attributed to the inherited limitations of the Holland model and the possible effect of mountains around Manila Bay which is not accounted in the model. In general, the simulated pressure and windspeed using the modified JTWC best track were able to estimate the observed values reasonably [44][45].

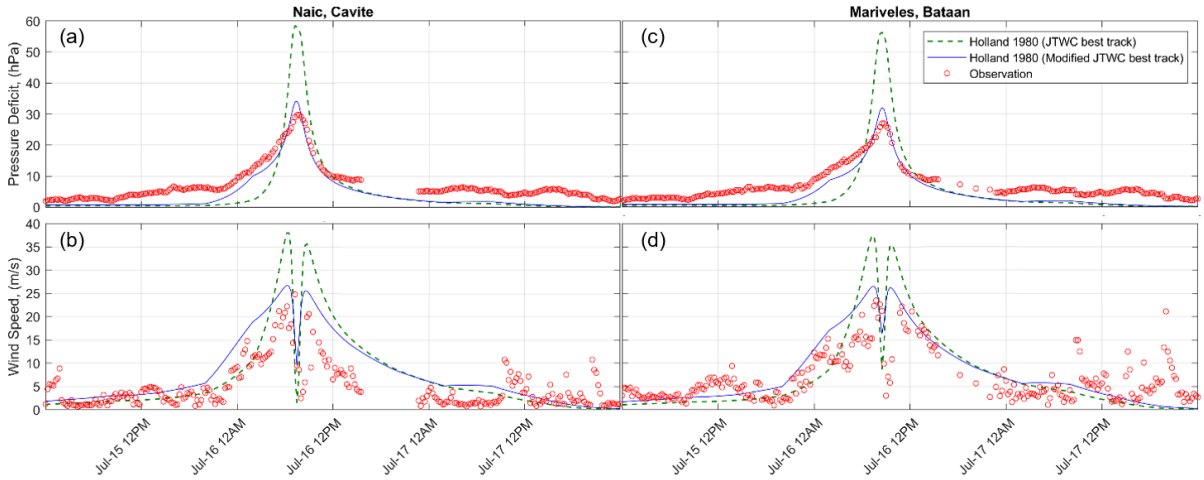

Figure 5. Comparisons of time series of (a and c) pressure deficit and (b and d) maximum 10-min sustained windspeed at 10-m elevation from the simulation using the JTWC best track and modified JTWC best track, and the observation at DOST-ASTI Naic, Cavite and Mariveles, Bataan stations.

2.3.3 Validation of Storm Surge

Illustrated in Figure 6 is the comparison of the time series of (a) observed water level and simulated tide and (b) modeled and observed storm surge at the NAMRIA Tide Station at Manila South Harbor from July 15-19, 2014. The observed water levels are reported in an hourly basis. The modeled storm surge (residual) was calculated by subtracting the simulated astronomical tide from the simulated water levels (storm tide) forced with the calibrated Typhoon Rammasun 2014 wind and pressure field. The observed storm surge was calculated using similar procedure – subtracting modelled astronomic tide from observed water level values. At the approach of the typhoon, there is a noticeable set-down of the simulated surge that is almost twice as that of the observed set-down. This set-down can be attributed when strong southwesterly winds are blowing outwards the bay. Simulated set-downs were also observed in the study of Tsai et al. (2020) in the semi-enclosed San Pedro Bay using the Holland wind model [46].

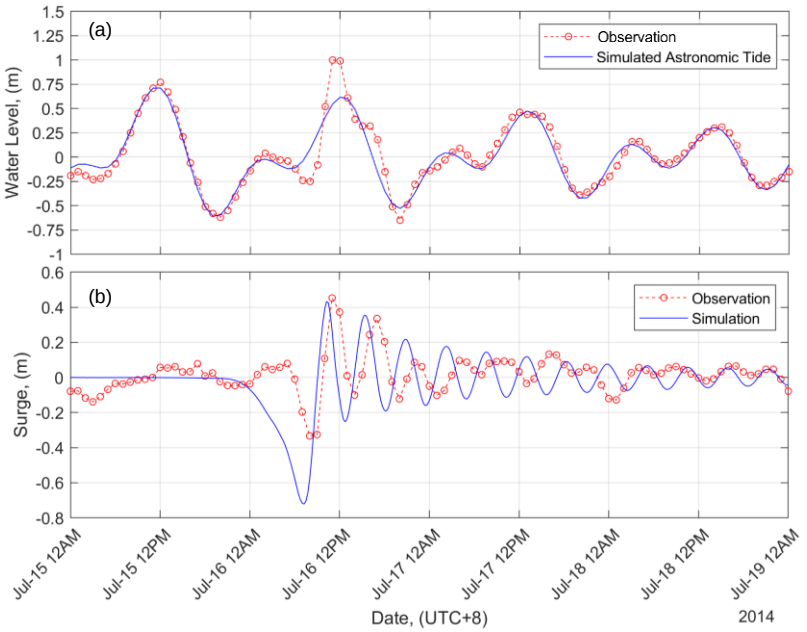

Figure 6. (a) Observed water level and simulated tide and (b) modeled versus observed storm surge at NAMRIA Tide Station, Manila South Harbor during Typhoon Rammasun 2014.

The observed peak storm surge occurred at 11:00 AM on July 16, 2014, while the simulated surge peaked earlier at 10:15 AM. The time difference of less than one hour is considered acceptable in storm surge simulation [10] and this is due to the 6-hourly typhoon positions of the best track data, and the positions are reported only up to 0.1 degree of latitude and longitude only – which translates to over 10 km within the latitude of Manila Bay. In terms of the peak values, the observed surge is 0.45 m while the simulated surge is 0.43 m which indicates a -4.7% difference. After the peak, there is an observed resonance effect in Manila Bay in both the simulated and observed surge curves. This bay seiche was also observed in the study of Morin et al. (2016) [15]. Overall, the modeled surge can satisfactorily reproduce the expected peak surge for the purpose of this study.

2.4 Variation of Tracks

Analysis of historical typhoon tracks was done to determine the characteristics of typhoon tracks that passed Manila Bay. To do this, typhoon tracks that traversed a 60 km search radius centered in Manila Bay (14.6°, 120.8°) covering the model domain were collected from the Japan Meteorological Agency (JMA) [47] and Joint Typhoon Warning Center (JTWC) from 1951-2021 [37]. A total of 30 typhoons were found and it was observed that there are three common typhoon path directions, namely, due Northwest (NW), due West (W), and due Southwest (SW). As expected, the due Northwest direction is the most frequent track (22 out of 30). The least common track is the due Southwest direction (1 out of 30).

In this study, we simulated the typhoon tracks for the three directions using the intensity of the calibrated Typhoon Rammasun 2014 and we used the same astronomical tide by maintaining the duration of the typhoon. For the due Northwest direction, Typhoon Rammasun 2014 was selected to be the reference track, also labeled as NW2. Tropical Cyclone (TC) Patsy

1970 and TC Teresa 1994 were used as references for the due West and due Southwest directions, respectively. In creating the typhoon tracks, the forward speed was kept the same for all the directions by maintaining the distance between the 6-hourly positions of the typhoon track, as referenced from TY Rammasun 2014 positions. Then to create the group of typhoon tracks, we shifted the reference track per direction vertically with an interval of 0.2 degrees latitude. Overall, there were 5 tracks per direction, and a total of 15 tracks for the three directions. Figure 7 presents the tracks that were simulated in this study – NW1-5 are tracks in the due Northwest direction; W1-5 are the tracks in the due West direction; and SW1-5 are the tracks in the due Southwest direction. The notation 1-5 is from lower latitude to higher latitude.

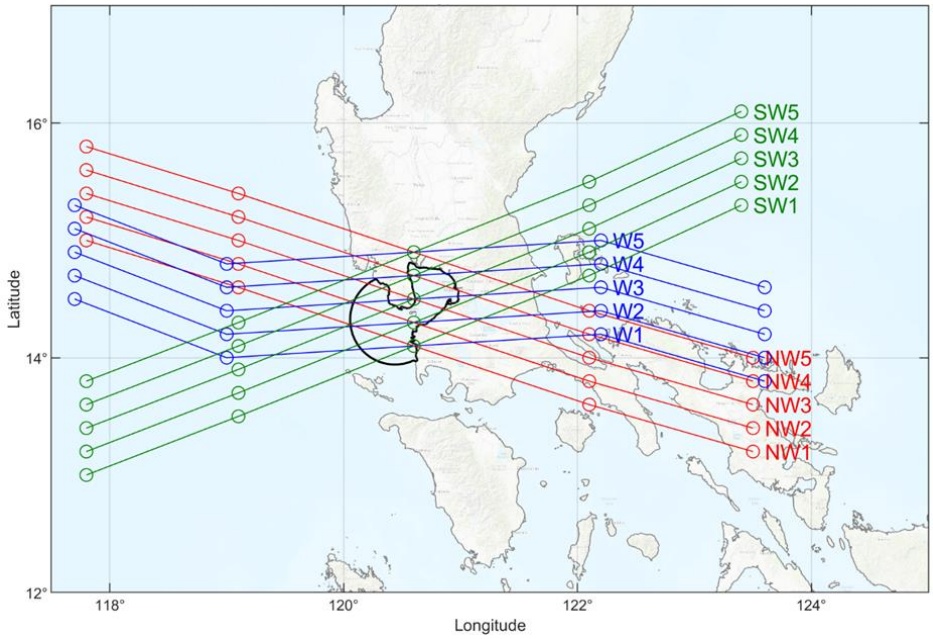

Figure 7. Paths of typhoons in the due Northwest direction (NW1-5) group, due West direction (W1-5) group, and due Southwest direction (SW1-5) group.

III. RESULTS

In this section, we present and discuss the results of the simulation of the groups of typhoon tracks in the three directions, namely due Northwest (NW1-5), due West (W1-5), and due Southwest (SW1-5) tracks. The typhoons were simulated from July 14-19, 2014, with the strength and forward speed of the calibrated Typhoon Rammasun (Glenda) 2014. The storm surge was calculated by subtracting the simulated astronomical tide from the simulated water levels (storm tide) at every recording time step and the peak storm surge was computed as the maximum storm surge at all time steps at any computational node in the domain.

3.1 Effect of typhoon tracks to surface and alongshore distributions

Illustrated in Figure 8 are the spatial distributions of the simulated peak storm surges in Manila Bay for all the typhoon tracks considered in this study. In general, we can see that the simulated peak storm surges increase from the opening of the bay to the inner portion of the bay. Also, it is observed that the highest simulated peak storm surge for all the tracks is

generated at the northern portion of the bay (Pampanga and northern Bataan coasts) where the bathymetry is shallow and mild sloping, and the coast is funneling in shape (Figure 2). We can also see that tracks outside of the bay generated relatively less storm surges as compared to tracks traversing inside of the bay. In addition, it can be seen that the highest peak surges for the three track groups are produced by NW3, W3, and SW3.

The derived alongshore distributions of peak storm surges along Manila Bay for all the tracks are shown in Figure 9. We can see that for all the tracks, the highest peak surges can be found at the Northern Bataan and Pampanga coastlines, except for SW1 track which produces its highest peak at the Bacoor Bay. In Bacoor Bay, a local maximum of peak storm surge can be observed that is apparent for tracks located south of Bacoor Bay (NW1, W1, SW1, NW2, W2 and SW2). Generally, NW tracks which are relatively perpendicular to the principal axis of the bay (Figure 2), generate the highest peak surges along Manila Bay coastlines as compared to W and SW tracks.

Here, we define the critical track as the track that produced the highest peak surge in Manila Bay. We can see in Figure 9 that NW3, W3 and SW3 tracks are the critical tracks in their respective group tracks. These typhoon tracks are found to pass through the Manila Bay directly, and their tracks traversed near the center of the bay (Figure 2 and Figure 8). Next to these tracks that produce relatively high storm surges are NW2, NW4, W4 and SW4. Except for NW2 track, these tracks traverse the inner portion of the bay. Also, we compare the alongshore distribution of peak storm surges of the critical tracks as presented in Figure 10. It can be observed that these three critical typhoons, while having different track orientations, can produce almost the same distribution of peak storm surges along Bataan coastline except for the highest peak storm surges at the northern part. Along the Cavite coastline, we also see similar peak surge distribution for the critical tracks except in Bacoor Bay. Along the Pampanga-Bulacan-Metro Manila coastline, different magnitudes of alongshore distributions are observed for the three critical tracks. This may be because Pampanga-Bulacan-Metro Manila coastline is facing the entrance and is exposed to longer fetches. Overall, the NW3 track produced the highest storm surges along Manila Bay compared to W3 and SW3 tracks.

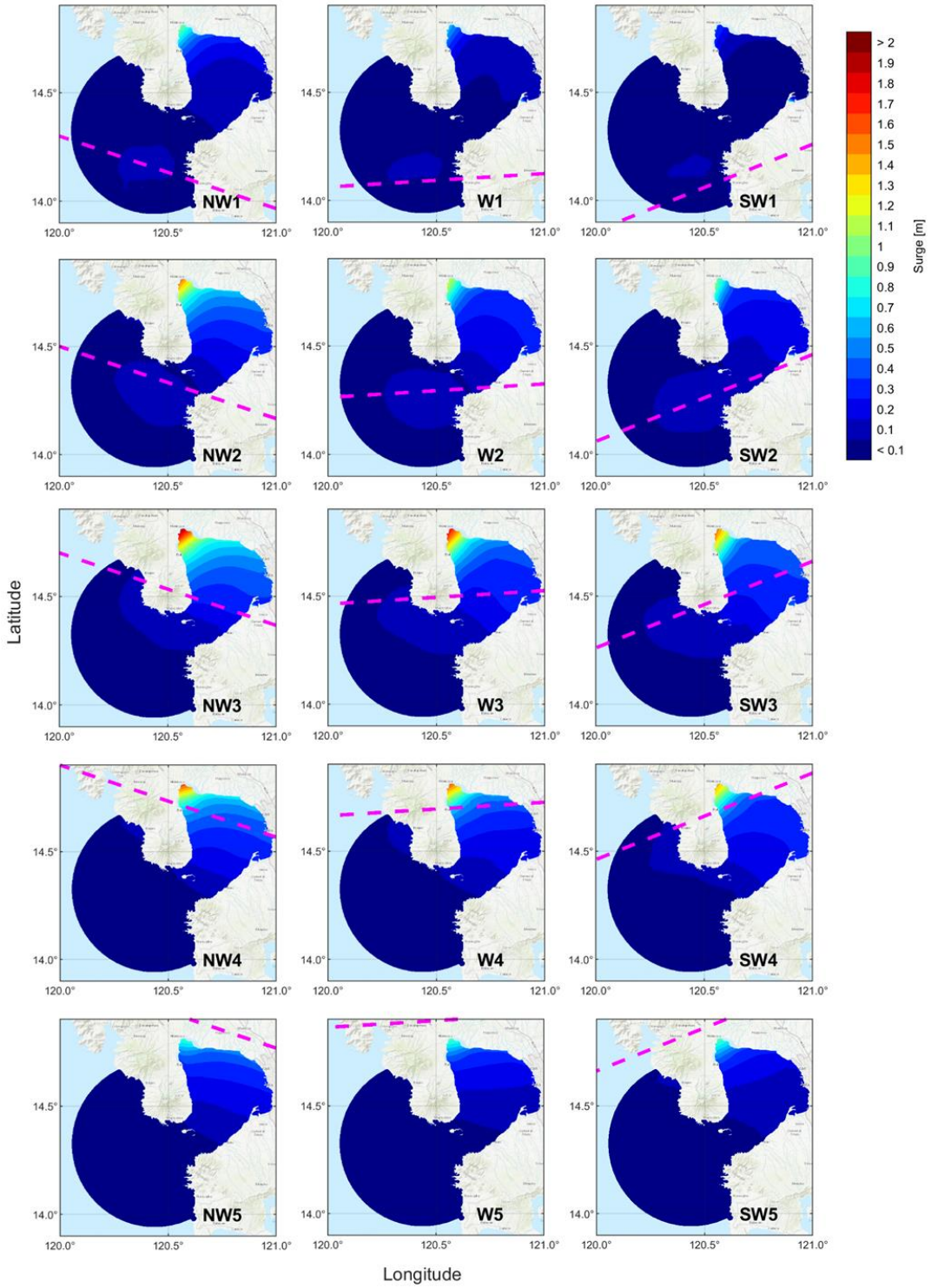

Figure 8. Spatial distributions of simulated peak storm surges in Manila Bay for the due Northwest (NW1-5) tracks (first column), due West (W1-5) tracks (second column) and due Southwest (SW1-5) typhoon tracks (third column). NW2 is the track of Typhoon Rammasun 2014.

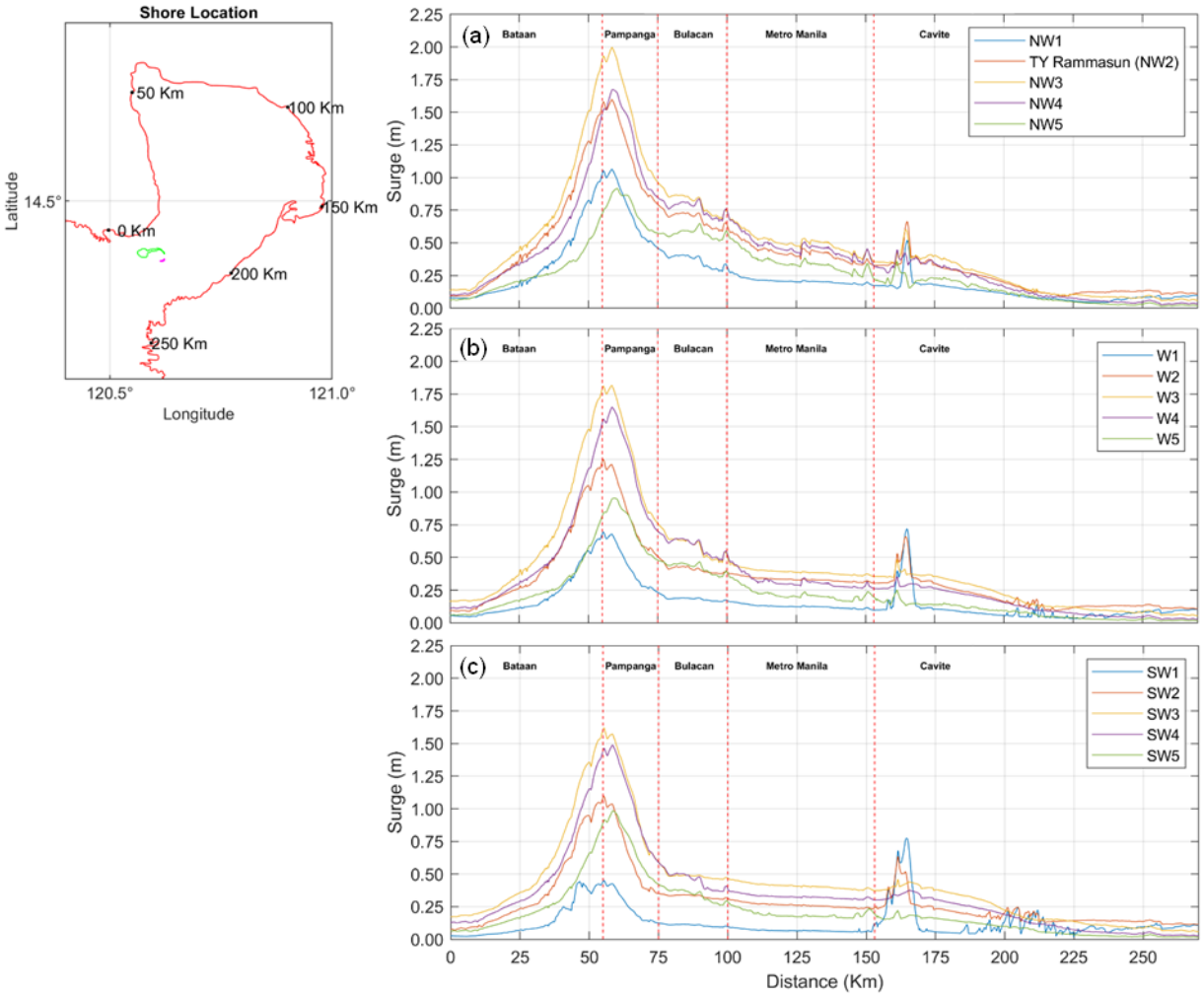

Figure 9. Alongshore distributions of simulated peak storm surge levels for the (a) Northwest (NW) tracks, (b) West (W) tracks, and Southwest (SW) tracks.

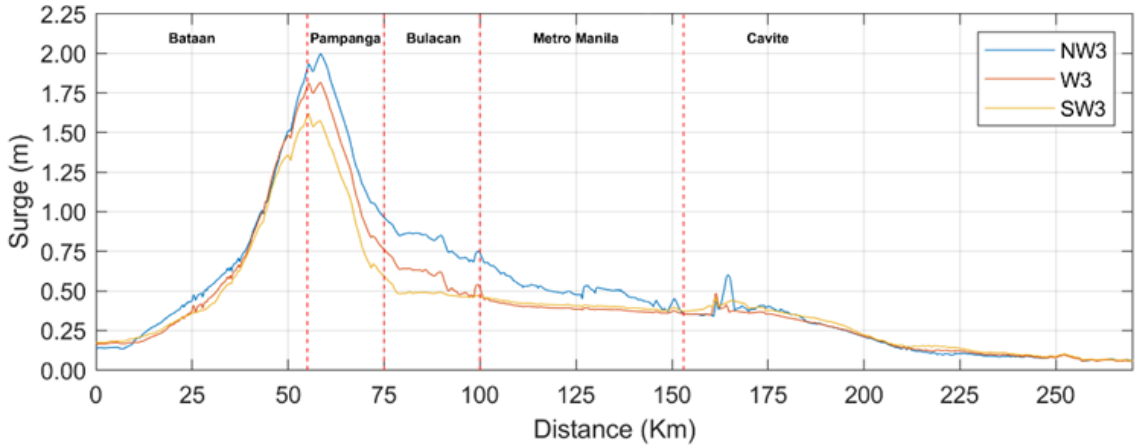

Figure 10. Comparison of alongshore distributions of simulated peak storm surges in Manila Bay for the most critical track per direction.

3.2 Effect of typhoon tracks on timing of surges

Figure 11 shows the instantaneous storm surge levels in time and in space (alongshore) for all the tracks. Generally, it appears that the same location of the tracks (i.e., tracks NW1, W1, SW1) with respect to Manila Bay produces similar distribution of instantaneous alongshore storm surges. We can see that storm surges start to peak first in Bacoor Bay than in other locations and then followed by a negative surge. Also, a negative surge before the peak surge is apparent along the Bulacan-Metro Manila coastline in the three group directions, especially for tracks 1-3.

Shifting of the tracks along the latitude affects the duration of storm surges. Longer duration but relatively low storm surges are observed along Bulacan-Metro Manila for tracks 4-5 in the three group directions. Tracks below Manila Bay (tracks NW1, W1, SW1) produce longer time to peak but relatively low magnitude of storm surges along the Northern Bataan and Pampanga coastlines. Storm surges along Bataan and Pampanga starts to rise before the storm surges along Bulacan-Metro Manila coastlines. Generally, the time for the surge to peak ranges from 1-3 hours along the coast of Manila Bay.

3.3 Effect of tides on surge height

The peak surge during Typhoon Rammasun coincided with high tide (Figure 6). To determine the effect of tides on storm surge height, we adjusted the timing of Typhoon Rammasun by 4 hours and then 8 hours so that the peak surge will occur at around mean tide level and at low tide, respectively. Figure 12a shows that simulated peak surges along the coasts are higher for low tides compared to high tides. However, the simulated peak storm tide levels at mean tide level are higher than both peak storm tide levels at high tide and low tide (Figure 12b).

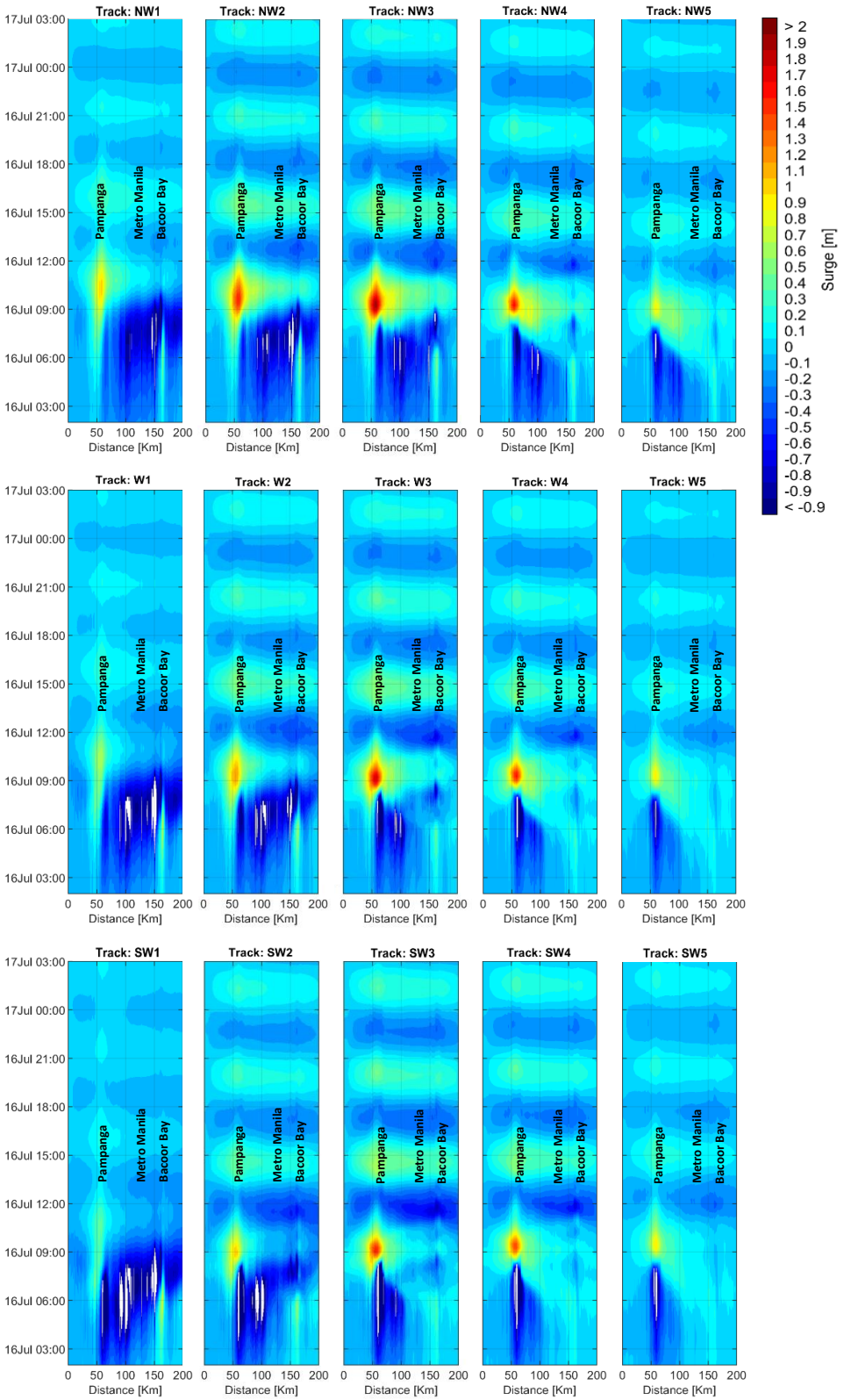

Figure 11. Comparisons of instantaneous storm surge levels in time and in space (alongshore) for all the tracks.

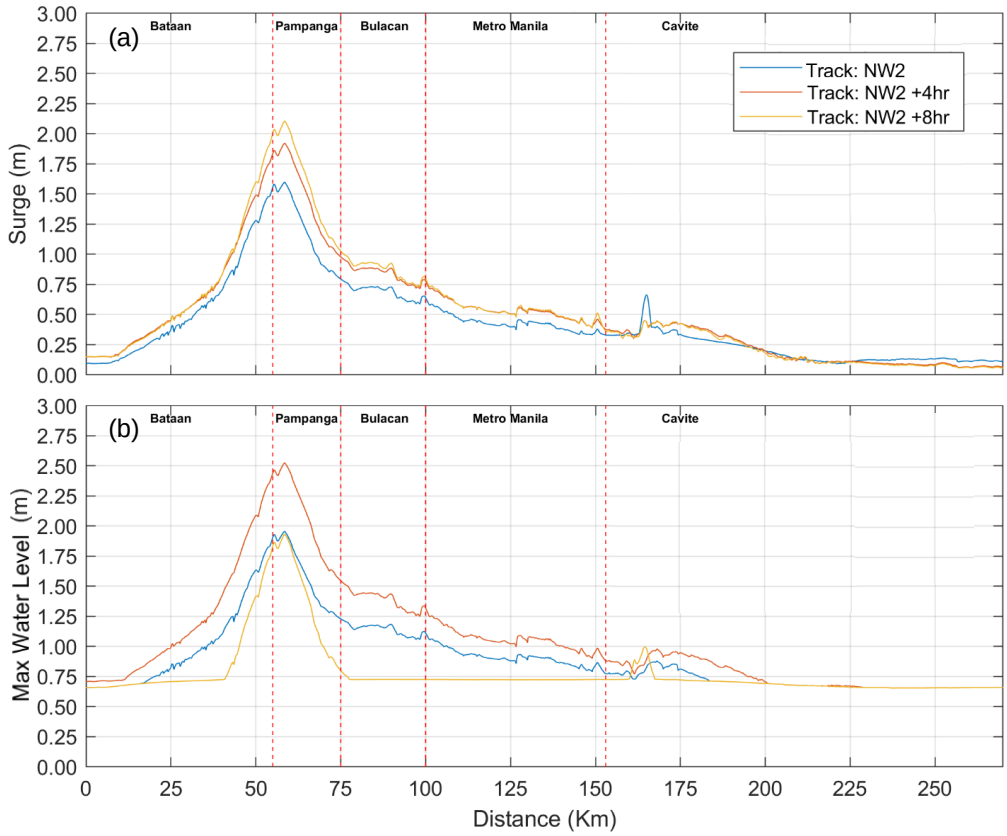

Figure 12. Comparison of alongshore distribution of simulated (a) peak surges and (b) peak water levels for high tide (NW2), mean tide level (NW2 +4hr), and low tide (NW2 +8hr)

3.4 Effect of different windspeeds

This study also investigated the effect of different windspeeds on storm surges using the NW3 track. We simulated constant windspeeds at 80, 100, and 120 knots representing Category 2, 3, and 4 typhoons based on the Saffir-Simpson Wind Scale, respectively. The corresponding pressures were determined based on Typhoon Rammasun data and the radius of maximum windspeed was set to a constant 20 nm. As expected, storm surges increase with increasing windspeed. Figure 13 shows the alongshore distribution of water levels at different windspeeds at mean tide level condition. We can see that the relative increase in water levels is highest at the Northern Bataan and Pampanga coastlines as compared to the relative increase in water levels near the mouth of the bay. This can be attributed to the shallow bathymetry and mild coastal slope along the Northern Bataan and Pampanga coastline and deep bathymetry and steep coastal slope near the mouth of the bay [7]. In Pampanga and Northern Bataan coasts, we can see that typhoons with maximum windspeeds of 80, 100, and 120 knots would reach potential highest water levels of 4.5 m, 5.0 m and 6.7 m, respectively.

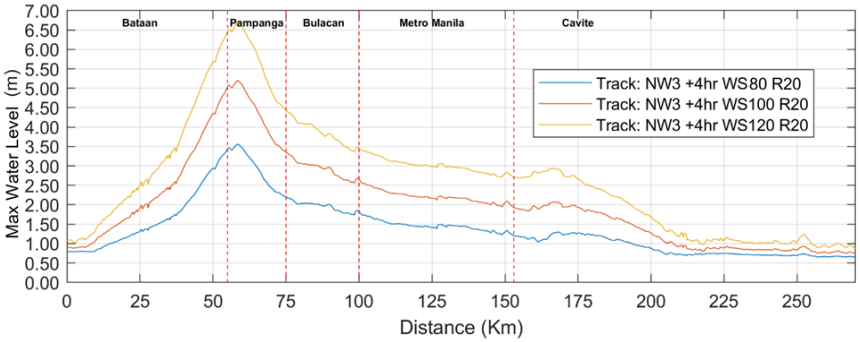

Figure 13. Comparison of alongshore distribution of simulated peak water levels for windspeeds 80 knots (blue), 100 knots (orange) and 120 knots (yellow) using a constant 20 nm Rmax at mean tide level condition for the NW3 track.

IV. CONCLUSION

Due to the growing urban population along the low-lying coastal areas in Manila Bay and its exposure to typhoons, this study aims to determine the effects of different typhoon tracks to storm surge response in Manila Bay. This paper used the ADCIRC model to numerically simulate the storm surges for different typhoon tracks. There were three track directions of typhoons traversing the Manila Bay area considered in the study, namely, due Northwest, due West, and due Southwest direction. The tracks were then shifted vertically by 0.2° latitude covering the Manila Bay area. There was a total of 5 tracks per direction simulated in this study with the forward speed and intensity of the calibrated TY Rammasun 2014.

Results of the study show that the magnitude of storm surges along the coast is affected by the track direction and shifting of the tracks. It is found that the due Northwest (NW) tracks, which are relatively perpendicular to the principal axis of the bay, produce the highest peak surge values as compared to the due West (W) and due Southwest (SW) tracks, while tracks located south of Bacoor Bay generate higher peak surges in Bacoor Bay. Critical tracks which produce the highest peak surges are found to be traversing near the geometric center of the bay (NW3, W3, SW3). The duration of the surge and the rise to peak surge along the Manila Bay coastlines are sensitive to the shifting of the typhoon tracks along the latitude. Longer duration of surges although relatively low in magnitude can be observed in tracks 4-5 in the three group directions along the Bulacan-Metro Manila coastline. In Bacoor Bay, peak surges occur first before peak surges in other coastlines.

Shifting of the tracks along the latitude in the due Northwest, due West and due Southwest directions affects the magnitude of the peak surges, however, this study also highlights that the characteristics of peak surge variation along the coast are influenced by the bathymetry, shape of the bay and coastline orientation [7][10]. Generally, the results of the simulation for all the tracks show that storm surge increase from the mouth of the bay (where the bathymetry is deep) to the inner bay along the Pampanga-Bulacan-Metro Manila coastline (where the bathymetry is shallow and the coastal slope is mild). Moreover, the highest peak surges can be found along the coasts of Northern Bataan and Pampanga where the coastal bathymetry is shallow, slope is mild, has a funneling coastline, and has the longest fetch for counterclockwise

winds. The orientation of Bacoor Bay, facing the northeast, is affected by the northeast winds from tracks approaching the bay which explains why storm surges occur first in Bacoor Bay. The Pampanga-Bulacan-Metro Manila coastline faces the entrance of the bay, thus, it is exposed to longer fetch for winds coming from the southwest. The relative increase of peak surges with respect to increase in windspeeds is higher in the inner bay coastlines as compared to the relative increase in peak surges near the mouth of the bay as the inner bay (Pampanga-Bulacan-Metro Manila coastlines) coast slope is along the bay primary axis slope. The results that tracks perpendicular to the principal axis produce the highest peak surges in the bay as well as critical tracks passing near the center of the bay are validation that the shape of Manila Bay affect the storm surge variation along the coast.

This research significantly improves the understanding of storm surge response in Manila Bay and in the effects of different typhoon tracks to storm surges in the bay. The study may be used for the assessment of coastal disasters and may aid in the design of mitigating measures.

V. DISCUSSION AND FUTURE WORK

This study focused on investigating the effects of typhoon tracks on storm surges in Manila Bay. Other typhoon parameters, such as forward speed, are also important to be investigated to understand their influence on storm surge generation in Manila Bay. Also, this study only investigated the storm surge generated by typhoons directly traversing the Manila Bay area. The effects of Southwest Monsoon enhanced by distant typhoons may be numerically investigated in the future as well. Based on the validation of the storm surge, it is observed that the simulated drawdown is greater than the observed drawdown. This may be attributed to the simulation of the wind field since orographic effects are not accounted by the Holland 1980 typhoon model. Other wind models aside from parametric models can also be explored such as the use of reanalysis wind fields. More importantly, the wind field can be created and corrected if there are sufficient available observed data onshore and along the coast. Additionally, the methodology employed in this research shifted the meteorological field directly and may not be able to keep dynamical characters when temperature and friction due to orographic effects are considered [48]. Furthermore, it is observed in this study that there is bay resonance in Manila Bay, however, it was not studied in detail as it is out of the scope of the study. In general, the simulated frequency of the bay is around 5-6 hours.

VI. ACKNOWLEDGEMENT

The authors would like to acknowledge the Department of Science and Technology – Advanced and Technology Institute (DOST-ASTI) for the observed wind and pressure data of Typhoon Rammasun (Glenda) 2014 and the National Mapping and Resource Information Authority (NAMRIA) for the surveyed bathymetric data of Manila Bay and the observed tides at the Manila South Harbor station. The lead author would also like to thank the Semirara Mining and Power Corporation for the support in this research through the Federico Puno Professorial Chair Award.

REFERENCES

[1] Cinco T, Guzman R, Ortiz A, Delfino R, Lasco, R, & Hilario F, Juanillo E, Barba R, Ares E. 2016. Observed trends and impacts of tropical cyclones in the Philippines. International Journal of Climatology. 36(14): 4638-4650.

[2] National Disaster Risk Reduction and Management Council (NDRRMC). 2013. Retrieved from: https://ndrrmc.gov.ph/attachments/article/1329/FINAL_REPORT_re_Effects_of_Typhoon_YOLANDA_(HAIYAN)_06-09NOV2013.pdf on September 12, 2021.

[3] Esteban M, Valenzuela V, Matsumaru R, Mikami T, Shibayama T, Takagi H, Thao D, De Leon M. 2016. Storm surge awareness in the Philippines Pior to Typhoon Haiyan: A comparative analysis with tsunami awareness in recent times. Coastal Engineering Journal. 58(1): 1640009-1-1640009-28.

[4] Perez R, Amadore L, Feir R. 1999. Climate change impacts and responses in the Philippines and coastal sector. Climate Research. 12:97-107.

[5] National Hurricane Center and Central Pacific Hurricane Center, National Oceanic and Atmospheric Administration. 2021. Retrieved from https://www.nhc.noaa.gov/surge/ on September 23, 2021.

[6] Bass B, Torres J, Irza J, Proft J, Sebastian A, Dawson C, Bedient P. 2018. Surge dynamics across a complex bay coastline, Galveston Bay, TX. Coastal Engineering. 138: 165-183.

[7] Mori N, Kato M, Kim S, Mase H, Shibutani Y, Takemi T, Tsuboki K, Yasuda T. 2014. Local amplification of storm surge by Super Typhoon Haiyan in Leyte Gulf. Geophysical Research Letters. 41: 5106-5113.

[8] Drews C. 2015. Directional storm surge in enclosed seas: The Red Sea, the Adriatic and Venice. Journal of Marine Science and Engineering. 3: 356-367.

[9] Bloemendaal N, Muis S, Haarsma R, Verlaan M, Apecechea MI, Moel H, Ward P, Aerts J. 2018. Global modeling of tropical cyclone storm surges using high resolution forecasts. Climate Dynamics. 52: 5031-5044.

[10] Zhang J, Xiong M, Yin C, Gan S. 2018. Inner shelf response to storm track variations over the east LeiZhou Peninsula, China. International Journal of Applied Earth Observation and Geoinformation. 71: 56-69.

[11] Liu X, Jiang W, Yang B, Baugh J. 2018. Numerical study on factors influencing typhoon-induced storm surge distribution in Zhanjiang Harbor. Estuarine, Coastal and Shelf Science. 215: 39-51.

[12] Ramos-Valle A, Curchitser E, Bruyère C. 2020. Impact of tropical cyclone landfall angle on storm surge along the Mid-Atlantic Bight. Journal of Physical Geophysical Research: Atmospheres. 125: 1-19.

[13] Tajima Y, Gunasekara K, Shimozono T, Cruz E. 2016. Study on locally varying inundation characteristics induced by Super Typhoon Haiyan. Part 1: Dynamic behavior of storm surge and waves around San Pedro Bay. Coastal Engineering Journal. 58(1): 1640002-1-1640002-29.

[14] Islam MR, Takagi H. 2020. Typhoon parameter sensitivity of storm surge in the semi-enclosed Tokyo Bay. Frontiers of Earth Science. 14: 553-567.

[15] Morin V, Warnitchai P, Weesakul S. 2016. Storm surge hazard in Manila Bay: Typhoon Nesat (pedring) and the SW monsoon. Natural Hazards. 81: 1569-1588.

[16] Camelo J, Cruz E, Cruz L. 2017. Simulative analysis of inland inundation behind Roxas Boulevard Seawall due to storm tide overtopping by historical typhoons. Asian and Pacific Coasts 2017; Manila Philippines. World Scientific Publishing. p. 364-375.

[17] Lapidez J, Tablazon J, Dsallas L, Gonzalo L, Cabacaba, K, Ramos M, Suarez J, Santiago J, Lagmay A, Malano V. 2015. Identification of storm surge vulnerable areas in the Philippines through the simulation of Typhoon Haiyan-induced storm surge levels over historical storm tracks. Natural Hazards and Earth System Sciences. 15:1473-1481.

[18] Sebastian A, Proft J, Dietrich C, Du W, Bedient P, Dawson N. 2014. Characterizing hurricane storm surge behavior in Galveston Bay using the SWAN+ADCIRC model. Coastal Engineering. 88: 171-181.

[19] Zou Q, Xie D. 2016. Tide-surge and wave interaction in the Gulf of Maine during an extratropical storm. Ocean Dynamics. 66: 1715-1732.

[20] Camelo J, Mayo T, Gutmann E. 2020. Projected climate change impacts on Hurricane storm surge inundation in the coastal United States. Frontiers in Built Environment. 6: 588049.

[21] Pringle W, Damrongsak W, Roberts K, Weterick J. 2021. Global storm tide modeling with ADCIRC v55: unstructured mesh design and performance. Geoscientific Model Development. 14: 1125-1145.

[22] Leuttich R, Westerink J, Scheffner N. 1992. ADCIRC: An Advanced Three-Dimensional Circulation Model for Shelves, Coasts, and Estuaries; Report 1: Theory and Methodology of ADCIRC-2DDI and ADCIRC 3-DL; Technical Report DRP-92 6; Department of the Army, USACE, Washington, DC, USA.

[23] Leuttich R, Westerink J. 2004. Formulation and Numerical Implementation of the 2D/3D ADCIRC Finite Element Model Version 44.XX, Technical report. University of North Carolina at Chapel Hill & University of Notre Dame.
[24] Garratt, J. 1977. Review of drag coefficients over oceans and continents. Monthly Weather Review. 105: 915-929.
[25] Holland G. 1980. An analytical model of the wind and pressure profiles in hurricanes. Monthly Weather Review. 108(8): 1212-1218.
[26] Gong J, Jia X, Zhuge W, Guo W, Lee DY. 2020. Assessment of a Parametric Tropical Cyclone Model for Typhoon Wind Modeling in the Yellow Sea. Journal of Coastal Research. 99: 67-73.
[27] Marsooli R, Lin N. 2018. Numerical modeling of historical storm tides and waves and their interactions along the U.S. East and Gulf Coasts. Journal of Geophysical Research: Oceans. 123: 3844-3874.
[28] Bao S, Xie L, Pietrafesa LJ. 2006. An asymmetric hurricane wind model for storm surge and wave forecasting. 27th Conference on Hurricanes and Tropical Meteorology; Monterey, California. American Meteorological Society. 9A.4.
[29] Peter Sheng Y, Yang K, Paramygin V. 2020. A rapid forecasting and mapping system of storm surge and coastal flooding. American Meteorological Society. 35: 1663-1681.
[30] Google Earth Pro version 7.3. 2021. Retrieved from https://www.google.com/earth/versions/ on July 19, 2021.
[31] General Bathymetric Chart of the Oceans (GEBCO). 2021. Retrieved from https://www.gebco.net/ on July 19, 2021.
[32] Garzon J, Ferreira C. 2016. Storm Surge Modeling in Large Estuaries: Sensitivity Analyses to Parameters and Physical Processes in the Chesapeake Bay. Journal of Marine Science and Engineering.
[33] Luma-ang C. 2019. The analysis of storm surges in Manila Bay, The Philippines. The International Hydrographic Review. 21: 7-20.
[34] Du M, Hou Y, Qi P, Wang K. 2020. The impact of different historical typhoon tracks on storm surge: A case study of Zhejiang, China. Journal of Marine Systems. 206: 103318.
[35] Egbert G, Erofeeva S. 2002. Efficient inverse modeling of barotropic ocean tides. Journal of Atmospheric and Oceanic Technology. 19(2): 183-204.
[36] National Disaster Risk Reduction and Management Council (NDRRMC). 2014. Retrieved from https://ndrrmc.gov.ph/attachments/article/1293/Effects_of_Typhoon_Glenda_(RAMMASUN)_Final_Report_16SEP2014.pdf on August 30, 2021.
[37] Joint Typhoon Warning Center (JTWC) Best Track Archive. 2021. Retrieved from https://www.metoc.navy.mil/jtwc/jtwc.html?best-tracks on July 19, 2021.
[38] Chu JH, Sampson CR., Levine AS, Fukada E. 2002. The Joint Typhoon Warning Center Tropical Cyclone Best-Tracks, 1945-2000 (Rep. NRL/MR/7540 02 16). Joint Typhoon Warning Center, HI.
[39] Philsensors. 2021. Retrieved from https://philsensors.asti.dost.gov.ph/site/data on August 9, 2021.
[40] Lopez, G.V. 2021. Personal communication, Senior Science Research Specialist, DOST-ASTI, on Aug 9, 2021.
[41] Newman J, Klein P. 2014. The impacts of atmospheric stability on the accuracy of wind speed extrapolation methods. Resources. 3: 81-105.
[42] Hardy T, McConochie, J, Mason, L. 2004. Modelling tropical cyclone over-water wind and pressure fields. Ocean Engineering. 31: 1757-1782.
[43] Department of Science and Technology - Philippine Atmospheric, Geophysical and Astronomical Services Administration. 2021. Retrieved from http://www.pagasa.dost.gov.ph/information/about-tropical-cyclone on September 12, 2021.
[44] Thomas A, Dietrich JC, Asher TG, Bell M, Blanton BO, Copeland JH, Cox, AT, Dawson CN, Fleming JG, Leuttich RA. 2019. Influence of storm timing and forward speed on tides and storm surge during Hurricane Matthew. Ocean Modelling. 137: 1 19.
[45] Yuxing W, Ting G, Ning J, Zhenyu H. 2020. Numerical study of typhoon parameters on the storm surge based on Hato storm over Pearl River Mouth, China. Regional Studies in Marine Science. 34: 101061.
[46] Tsai Y, Wu TR, Lin C, Lin S, Yen E, Lin C. 2020. Discrepancies on storm surge predictions by parametric wind model and numerical weather prediction model in a semi-enclosed bay: case study of Typhoon Haiyan. Water. 12(12): 3326.
[47] Japan Meteorological Agency Best Track Database. 2021. Retrieved from https://www.jma.go.jp/jma/jma-eng/jma-center/rsmc-hp-pub-eg/besttrack.html on July 19, 2021.

[48] Yasuda T, Mori N, Nakajo S, Mase H, Hayashi H, Oku Y. 2011. Projection of future storm surge due to climate change and its uncertainty – a case study in the Tokyo Bay. Sixth International Conference on Asian and Pacific Coasts (APAC) 2011; Hongkong China. World Scientific Publishing. p. 369-376.